Adapting a Compact Confocal Microscope System to a Two-Photon Excitation Fluorescence Imaging Architecture

ALBERTO DIASPRO[1]*, MIRKO COROSU,[1] PAOLA RAMOINO,[2] AND MAURO ROBELLO[1]
[1]*INFM and Department of Physics, University of Genoa, 16146 Genova, Italy*
[2]*DIP.TE.RIS., University of Genoa, 16124 Genova, Italy*

KEY WORDS two-photon microscopy; single-pinhole confocal microscopy; three-dimensional point-spread function; helical biostructure; 3D imaging

ABSTRACT Within the framework of a national National Institute of Physics of Matter (INFM) project, we have realised a two-photon excitation (TPE) fluorescence microscope based on a new generation commercial confocal scanning head. The core of the architecture is a mode-locked Ti:Sapphire laser (Tsunami 3960, Spectra Physics Inc., Mountain View, CA) pumped by a high-power (5 W, 532 nm) laser (Millennia V, Spectra Physics Inc.) and an ultracompact confocal scanning head, Nikon PCM2000 (Nikon Instruments, Florence, Italy) using a single-pinhole design. Three-dimensional point-spread function has been measured to define spatial resolution performances. The TPE microscope has been used with a wide range of excitable fluorescent molecules (DAPI, Fura-2, Indo-1, $DiOC_6(3)$, fluoresceine, Texas red) covering a single photon spectral range from UV to green. An example is reported on 3D imaging of the helical structure of the sperm head of the Octopus *Eledone cirrhosa* labelled with an UV excitable dye, i.e., DAPI. The system can be easily switched for operating both in conventional and two-photon mode. *Microsc. Res. Tech. 47:196–205, 1999.*

INTRODUCTION

Among the most important and well-established advances in the field of microscopy, confocal laser scanning microscopy (CLSM) plays a fundamental role (Benedetti, 1998; Wilson, 1990; Wilson and Sheppard, 1984;). CLSM allows penetratation of the very intriguing three-dimensional (3D) properties of biological systems to study the delicate and complex relationship existing between structure and function in the biological systems (Brakenhoff et al., 1986; Diaspro et al., 1996). The advent of two-photon excitation (TPE) in fluorescence microscopy dramatically enhanced the field of action of CLSM (Denk et al., 1990; Piston, 1999). The application of TPE to fluorescence microscopy has stimulated a continuously growing number of fabulous and terrific opportunities (Hell, 1996; Potter, 1996). One of the outstanding and appreciated applications of fluorescence microscopy is to simultaneously image various bio-structures in a single cell studied under favourable physiological conditions (Pawley, 1995). In classical fluorescence microscopy, distinct bio-structures within the cell are labelled with specific fluorescent probes. In general, fluorescent probes have separated absorption spectra and each bio-structure can be selectively excited by using the proper excitation wavelength. The spatial relationship between these bio-structures can be determined by superimposing a series of images collected with multiple excitation wavelengths (Beltrame et al., 1995). Moreover, optical sectioning ability extends this capability to the whole volume of the cell (Agard, 1984; Wilson and Sheppard, 1984). Unfortunately, the 3D process adds the problem that the sample is subjected to multiple and long exposures that may cause significant photo-damage. These concerns can be greatly alleviated by using TPE (Potter, 1996). The single quantum event allowing TPE was predicted in 1931 (Göppert-Mayer, 1931) and experienced only in 1961, after the advent of the laser (Kaiser and Garret, 1961). To date, the application of TPE to scanning optical microscopy was pointed out by the Oxford Group in 1977 (Gannaway and Sheppard, 1978; Sheppard and Kompfner, 1978; Wilson and Sheppard, 1979). Successively it was operatively introduced at the WW Webb laboratories (Cornell University, Ithaca, NY) in the 1990s (Denk et al., 1990). As reported by S.W. Hell (Hell, 1996), almost 3 years after its first demonstration at WW Webb laboratories, Webb himself noticed the fact that, in spite of TPE relative simplicity, no other laboratory had pursued TPE imaging.

Nowadays, there are two popular approaches to realise TPE imaging architectures. The first approach uses the very same optical pathway and mechanism employed in CLSM. Pinholes are removed or set to their maximum aperture and the emission signal is captured using the galvanometric scanning mirrors. This is called de-scanned mode. The other approach is called non-de-scanned mode. In non-de-scanned mode, the CLSM optical path is modified in order to increase signal-to-noise ratio and pinholes are removed. The emitted radiation is collected using dichroic mirrors on the emission path or external detectors without passing through the galvanometric scanning mirrors (Denk et al., 1995). In order to obtain a better spatial resolution, it is also possible to keep confocal pinholes. Unfortunately, in some practical experimental situations, the

Contract grant sponsor: INFM.

*Correspondence to: Alberto Diaspro, Department of Physics, University of Genova, Via Dodecaneso 33, 16146 Genova, Italy.

Received 13 July 1999; accepted in revised form 28 July 1999

low efficiency of TPE fluorescence process may rule out such a solution. However, when pinhole insertion is possible, the major advantage is attained in terms of better axial resolution approximated at 40% (Gu and Sheppard, 1993; Higdon et al., 1999; Nakamura, 1993).

In TPE, two infrared photons must collide with a fluorescent molecule simultaneously. This means that fluorescent molecules have to absorb two photons per excitation event having half the energy needed for the excitation transition. Under this circumstance, fluorescence depends on the square of the infrared light intensity and consequently decreases with the inverse fourth power of the distance from the focus volume allowing depth discrimination (Cannel and Soeller, 1997). For conventional excitation, in a spatially uniform fluorescent sea, equal fluorescence intensities are contributed from each optical slice above and below the actual in the realistic assumption of negligible excitation attenuation (Wilson and Sheppard, 1984). In TPE over the 80% of the total intensity of fluorescence comes from a 700–1,000-nm-thick region about the focal point for objectives with numerical apertures in the range from 1.2 to 1.4. This is the intrinsic confocal effect due to TPE. Moreover, the dramatic reduction of background in TPE imaging allows compensating for the reduction in spatial resolution (Denk et al., 1995; Centonze and White, 1998). This reduction is due to the larger diffraction limited spot with respect to the conventional case where half the wavelength is used (Born and Wolf, 1993; Nakamura, 1993). In principle, in a dark room, where a TPE experiment takes place, one should acquire all the radiation at the wavelength of fluorescence emission being excited. In fact, the excited volume localisation is strictly dependent on the selective excitation of the actual imaged volume allowing the utilisation of large area detectors. Since TPE occurs only at a region of high temporal and spatial concentration of photons, high numerical focusing objectives (approximately 1.2–1.4 NA) and high power pulsed laser sources are needed together. While for the former requirement the situation is well established, for the latter only the advent of femtosecond mode-locked laser sources dramatically changed and simplified the situation. For typical cross-sections of the order of 10^{-58}–10^{-52} m^4 s/photon/molecule, a 100-fs pulsed infrared laser operating at 80 MHz of repetition rate at an average power of 50 mW can prime the TPE process (Denk et al., 1990). In practice, the energy needed is less considering all the sources of loss and of degradation along the optical path from the source to the sample (Pawley, 1995). Recently, the cross-section parameter has been measured for a wide range of dyes (Xu and Webb, 1996). Furthermore, new "ad hoc" organic molecules, endowed with large two-photon absorption cross-sections, have been developed (Albota et al., 1998).

We will show that it is fairly straightforward, under some circumstances, to adapt a new generation compact scanning head for TPE imaging (Diaspro and Robello, 1999; Potter, 1996; Soeller and Cannel, 1996). In particular, one does need a stable and easy-to-use laser source and a very good confocal scanning head with the additional property of a simple but effective head design. Within the framework of a national project of the National Institute of the Physics of Matter (INFM), we have recently realised a TPE fluorescence microscope, part of a multipurpose architecture including also lifetime imaging and fluorescence correlation spectroscopy modules (So et al., 1996; Systma et al., 1998). Figure 1 presents a view of the TPE architecture operating in our laboratory.

TPE ARCHITECTURE.

Because TPE is still a young, even if mature and quickly growing, technique we decided to realise an architecture based on an affordable commercial confocal scanning head. We tested the performances and the quality/cost ratio for different systems and at the end of the process we elected the new Nikon scanning head, i.e., PCM2000 (Nikon Instruments, Florence, Italy), as the core of our system. This head presents a very simple and efficient design, formerly known as BRITE*i (Pawley, 1995). The main architectural characteristics are a high compactness, the utilisation of a single-pinhole optical path, and an all fiber system for excitation and emission delivery of light. The PCM2000 scanning head employs self-aligning confocal optics that allows changing excitation filters, barrier filters, and even the primary excitation dichroic filter without the need of alignment procedures. This is due to the all-fiber system that serves as both the source and the pinhole. The fluorescence signal at each pixel is detected by standard photomultiplier tubes (R928, Hamamatsu, Japan). The objective axial position is driven by two different computer interfaced devices, namely: a belt-driven system using a DC motor allowing 0.1-μm steps (RFZ-A, Nikon, Japan) and a single objective piezo nano-positioner (PIFOC P-721–17, Physik Instrumente PI, Germany). The piezo positioner allows an axial resolution of 0.01 μm with a range of 100 μm and utilizes a linear variable differential transformer (LVDT) integrated feedback sensor. The experimental lateral and axial Full Width at Half Maximum (FWHM) resolution parameters, in conventional fluorescence excitation mode, have been evaluated as 178.4 ± 20.9 nm and 508.6 ± 49.4 nm, respectively (Diaspro et al., 1999). These data are in agreement with the theoretical values of 180 and 480 nm, for the lateral and axial FWHM calculated, using Huygens2 (Scientific Volume Imaging, The Netherlands), by means of electromagnetic diffraction theory (Born and Wolf, 1993). Moreover, coupling image restoration schemes, we were also able to operate in the subresolution regime (data not shown; Bertero and Boccacci, 1998; Schrader et al., 1996; van der Voort and Strasters, 1995). Acquisition and visualisation are computer controlled by EZ2000 (Coord, The Netherlands) dedicated software. The ics-ids standard for image storage is used (Dean et al., 1990). Image export is guaranteed in any common image format.

The laser used in our TPE architecture is a modelocked Titanium-Sapphire (Ti-Sapphire) laser (Tsunami 3960, Spectra Physics, Mountain View, CA) pumped by a high power (5W at 532 nm) solid state laser (Millennia V, Spectra Physics). The features of this laser are high average power, 80 MHz high repetition rate, and 100 fs short pulse width. High peak power is critical for efficient photon excitation and consequently average power, related to it by the duty cycle ($P_{average} \approx D^*P_{peak}$; D= (pulse length) multiplied by (repetition rate)).

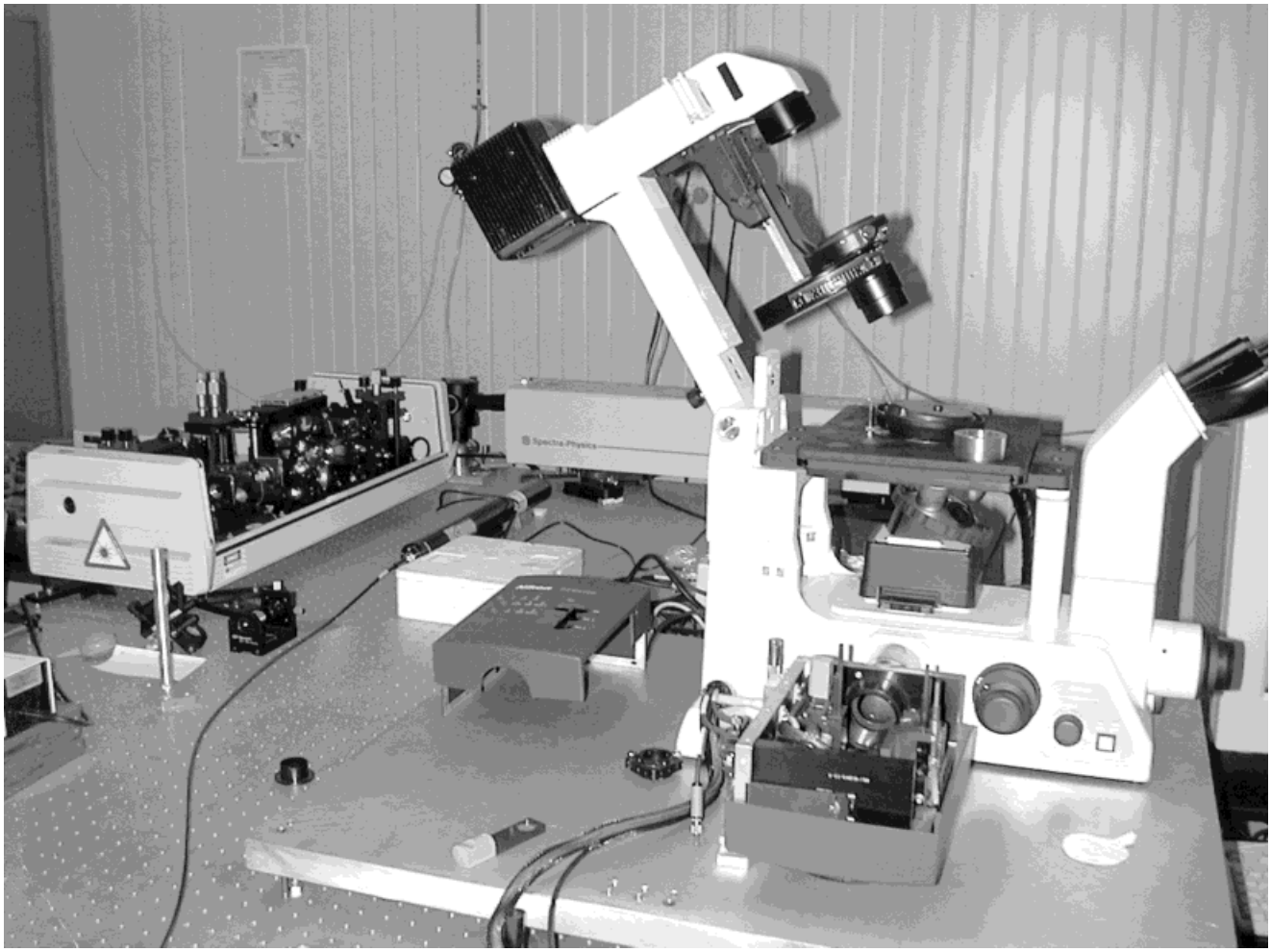

Fig.1.
TPE microscope operating as national facility of the National Institute of the Physics of Matter; see Figures 3 and 4 for details. **Left:** The opened cavity of Tsunami. **Right:** The opened PCM2000 confocal scannng head plugged into the lateral port of the inverted microscope.

The Tsunami laser source has a typical rms noise less than 0.5% and a percent power drift inferior to 5% in any 2-hour period with less than ± 2°C temperature change after a 1-hour warm-up. The Ti-Sapphire laser has a tuning range from 650 to 1,050 nm corresponding to conventional fluorescence excitation wavelengths from 325 to 525 nm. Our system operates in optimal conditions with wavelengths ranging from 680 to 830 nm. This is due to the specific set of mirrors we installed. In detail, we measured a pulse width below 90 fs in the 680–830 spectral range allowed by our mirror set and an average power until 800 mW in the central spectral region (Fig. 2). Tsunami polarization is vertical (>500:1) and the beam divergence is <0.6 mrad. Recently a new mirror set has become available covering almost all the Ti-sapphire spectrum. To date, most TPE microscopy data have been conducted using excitation wavelengths from 720 to 800 nm. The longer wavelengths are also used since cellular protein absorption is significantly lower and cellular auto-fluorescence is greatly reduced. Moreover, photodamage is also reduced at longer wavelengths (Konig et al., 1997, 1999). For sake of completeness, it has to be reported that a limiting factor for operating at long wavelengths is the one imposed by the spectral absorption windows of water. The 80 MHz laser output pulse is controlled by an internal fast photodiode that provides feedback signals for keeping the cavity length constant. Furthermore, the output of the photodiode is used as a phase locking signal and is available at the output at its own frequency and divided by eight (i.e., 10 MHz). The module that controls these operations is a Lok-to-clok (model 3930, Spectra Physics) accessory that is particularly useful also for lifetime measurements (So et al., 1996; Systma et al., 1998).

An overall schematic view of the architecture is reported in Figure 3. Before being directed to the PCM2000 compact scanning head, mounted on a TE300 (Nikon Instruments, Italy) inverted microscope, the beam is brought to an average power ranging from 20 to 40 mW utilising variable neutral density filters (CVI, CT). Moreover, a low magnification and low numerical aperture objective lens is placed at the entrance port of the scanning head, miming the optical characteristics

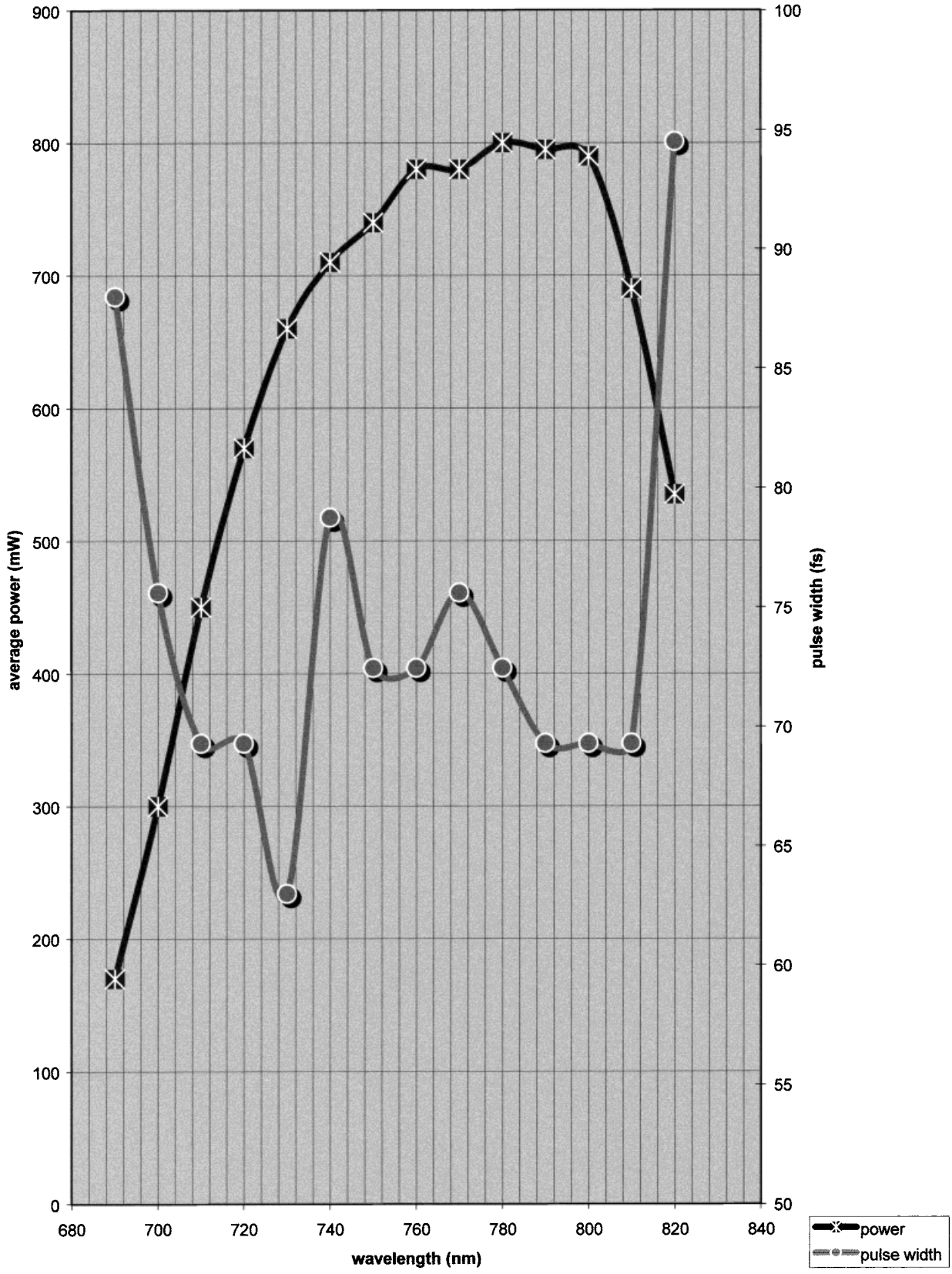

Fig. 2. The average power and pulse-width characteristics of the laser source. The source is a Tsunami model (Spectra Physics, Mountain View, CA), IR mode-locked pulsed laser pumped by a very efficient and simple-to-use solid-state green pump (Millennia 5 W model; Spectra Physics). Measurements have been conducted using an RE201 model ultrafast laser spectrum analyzer (Ist-Rees, UK), and a AN2/10A-P model thermopile detector power meter (Ophir, Israel). A trial Model 409–08 scanning autocorrelator (Spectra- Physics) has been used for pulse width measurements. The autocorrelator, which allows signal display on a high-impedance oscilloscope, can be used, over the wavelength range from 650 to 1,600 nm, to measure pulse widths from 25 ps to $<$80 fs, by changing the modules. To compensate pulse broadening from materials, a similar setup using two high-index prisms is used and is all that is necessary.

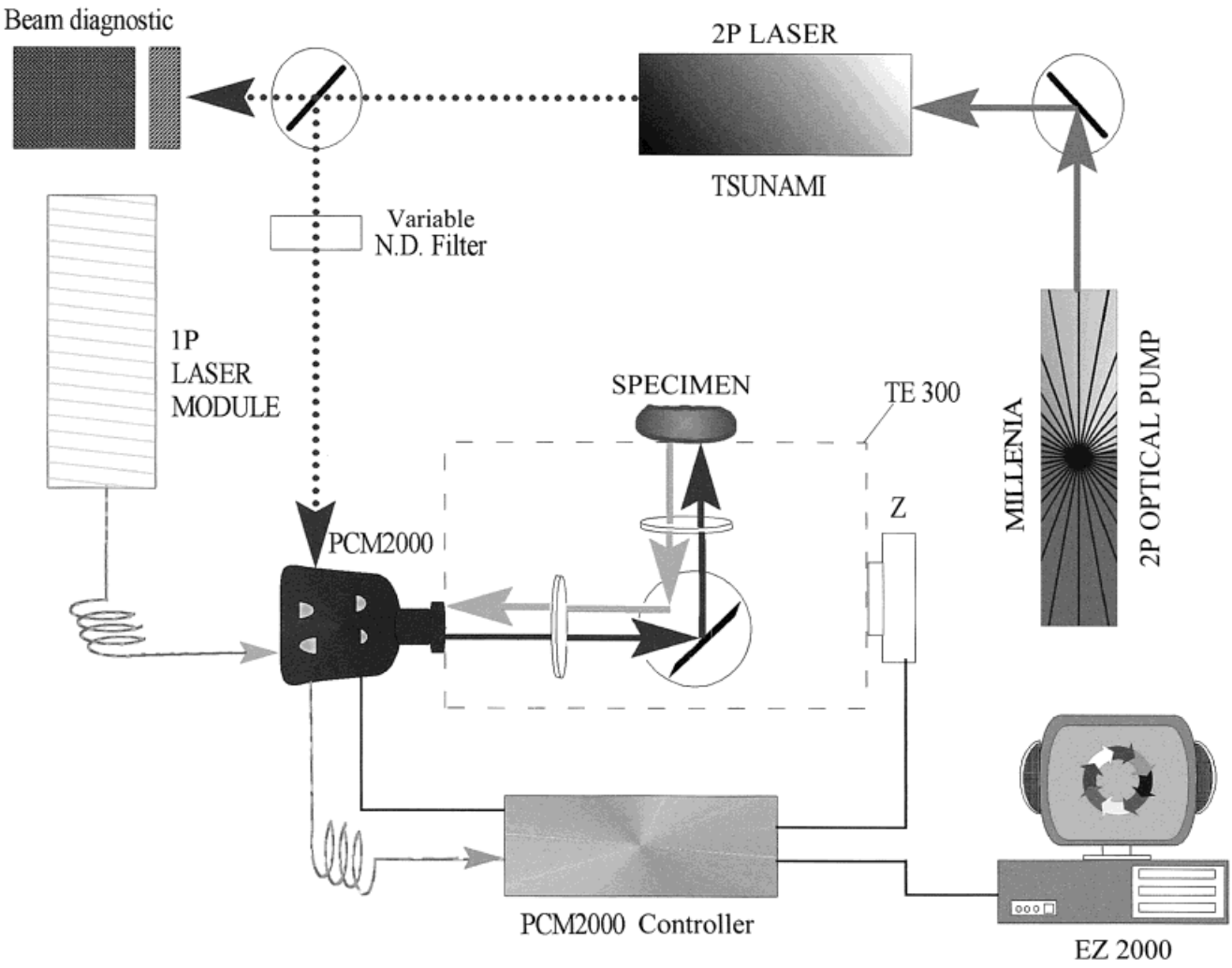

Fig. 3. Schematic drawing of the TPE confocal laser scanning microscope using the single pinhole PCM2000 scanning head coupled to conventional (1P) and pulsed laser (2P) sources. The excitation at PCM2000 input can be easily switched to single photon excitation using single-mode fiber delivery. Dichroics, pinholes, and filters can be inserted or removed using manual sliders. PCM2000 electronics, governing scanning and acquisition, is completely computer controlled. Beam diagnostics is performed using an ultrafast laser spectrum analyzer RE201 (Ist-Rees, UK) and a thermopile detector power meter AN2/10A-P (Ophir, Israel).

of the optical fiber usually placed at this entrance in conventional confocal mode (Fig. 4). This objective lens allows the utilization of the scanning head optical path without further modifications. In order to optimize the optical situation, a dichroic mirror has been substituted in the original scanning head to allow excitation from 680 to 1,010 nm (Chroma Inc.) and a special emission filter E650SP (Chroma Inc.) has been introduced on the emission path before output optical fibers in order to reject stray light. The E650SP filter blocks IR (infrared, i.e., $>$ 650 nm) excitation to an OD (optical density) of 6–7, operating at its best performances until 50 mW of impinging power beam. A new Nikon 100x/1.4 NA oil immersion IR objective is used, and the scanning head operates in the "open pinhole" condition, i.e., a large aperture that does not produce the classical confocal plane selection effect. The PCM2000 optical path is modified to perform "non-descanned" acquisition by introducing two dichroic mirrors for a direct coupling of the fluorescence coming from the sample to the optical fiber output channels (Fig. 4). This last section for non-de-scanned acquistion is still in progress in terms of evaluation of S/N behaviour and for correcting beam displacements introduced by inserting optical components along the optical path.

One-photon to two-photon mode switching is simply obtained by inserting a mono-mode optical fiber coupled to conventional laser sources for one-photon and by accessing the very same scanning head input channel directly from Tsunami when operating in the TPE mode. In both cases, i.e., conventional and TPE confocal, an optical fiber delivers the emitted fluorescence to the PCM2000 control unit where photomultiplier tubes are physically plugged.

The quadratic dependence on the excitation intensity, which forms the basis for the application of TPE for 3D microscopy, has been checked for a solution of fluoresceine (Merck, Germany) in water. All intensity

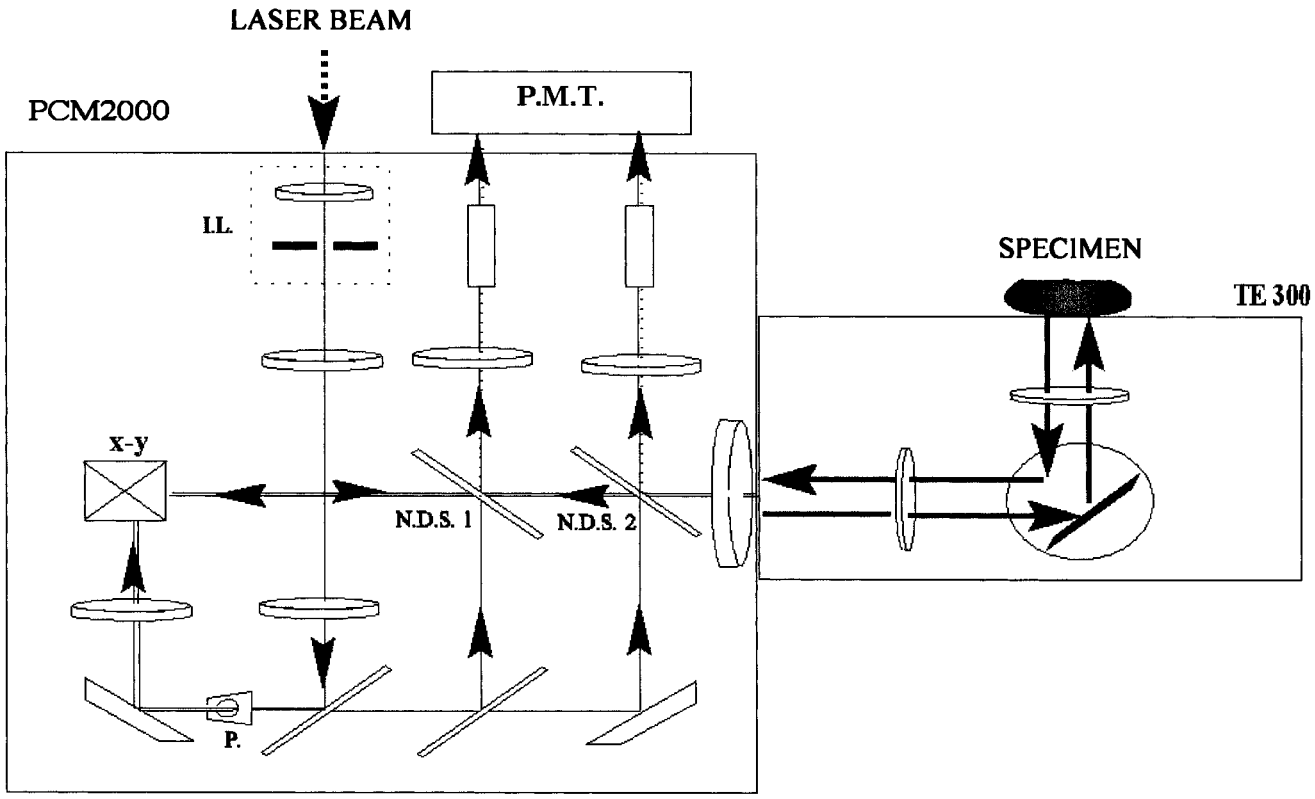

Fig. 4. Details of the coupling between the PCM2000 scanning head and the Tsunami laser source. Input lens (I.L.), single pinhole aperture (P.), galvanometric mirrors (x-y), and non-de-scanned mode dichroics (N.D.S.1, N.D.S.2) optical positions are visible. See text for further details.

data, corrected only for background and measured in the central subarea of the scanned region, fell within a logarithmic best-fit straight line that has a slope of 1.9996 (R = 0.9965).

The quadratic behaviour may be also considered a useful check of TPE conditions. Moreover, another test for checking TPE condition is given by the disappearance of fluorescence emission when de-pulsing the beam.

RESULTS

To characterise the spatial resolution of the TPE system, blue fluorescent carboxylate modified microspheres 0.1 μm diameter (F-8797, Molecular Probes, Eugene, OR) were used. A drop of dilute samples of bead suspensions was spread on a coverslip of nominal thickness 0.17 mm and air dried in a dust clean chamber. These microspheres constitute a very good compromise towards the utilization of subresolution point scatterers and acceptable fluorescence emission given the expected resolution of TPE. We excited an 18 × 18 μm field, at 720 nm at a pixel dwell time of 17 μs and a laser average power of 20 mW at the entrance of the scanning head.

We imaged 21 z-sections of fluorescent beads with z-scan steps of 0.1 μm. The x-y scan step was 0.035 μm. The PCM2000 pinhole was set to open position. The 3D images of 10 microspheres were analyzed.

The measured FWHM radial and axial resolution were 0.21 and 0.7 μm, respectively. They are in agreement with the prediction of Fraunhofer diffraction approximation. Experimental data and theorethical expectations are reported in Figure 5. Our results indicate that compact and simple commercial scanning heads perform well when adapted to TPE imaging. Using the measured instrumental point-spread function, images of complex biostructures can be further sharpened using deconvolution methods coupled to known point-spread function (Bertero and Boccacci, 1998; Castleman, 1996). We are working on this approach to improve the TPE resolution of complex cellular biostructure images.

An example of TPE imaging is given in the study of the structure of sperm heads of the Octopus *Eledone cirrhosa*. The sample has been prepared according to previously published procedures (Diaspro et al., 1997). We used an UV excitable fluorescent dye, i.e., DAPI (4',6-diamidino-2-phenylindole hydrocloride) (Matsumoto et al., 1981), to visualize the helical structure in a 3D framework. We excited the sample with a laser power of 20 mW, at a wavelength of 720 nm, on a 70 μm^2 field (Gryczynski et al., 1996).

Figure 6 shows 12 sections sampled from a stack of 64, 512 × 512 × 8 bits, taken 0.2 μm apart along the optical axis. The dimensions of the sperm head are pitch = 0.6–0.75 μm, outer radius = 0.25–0.3 μm, and

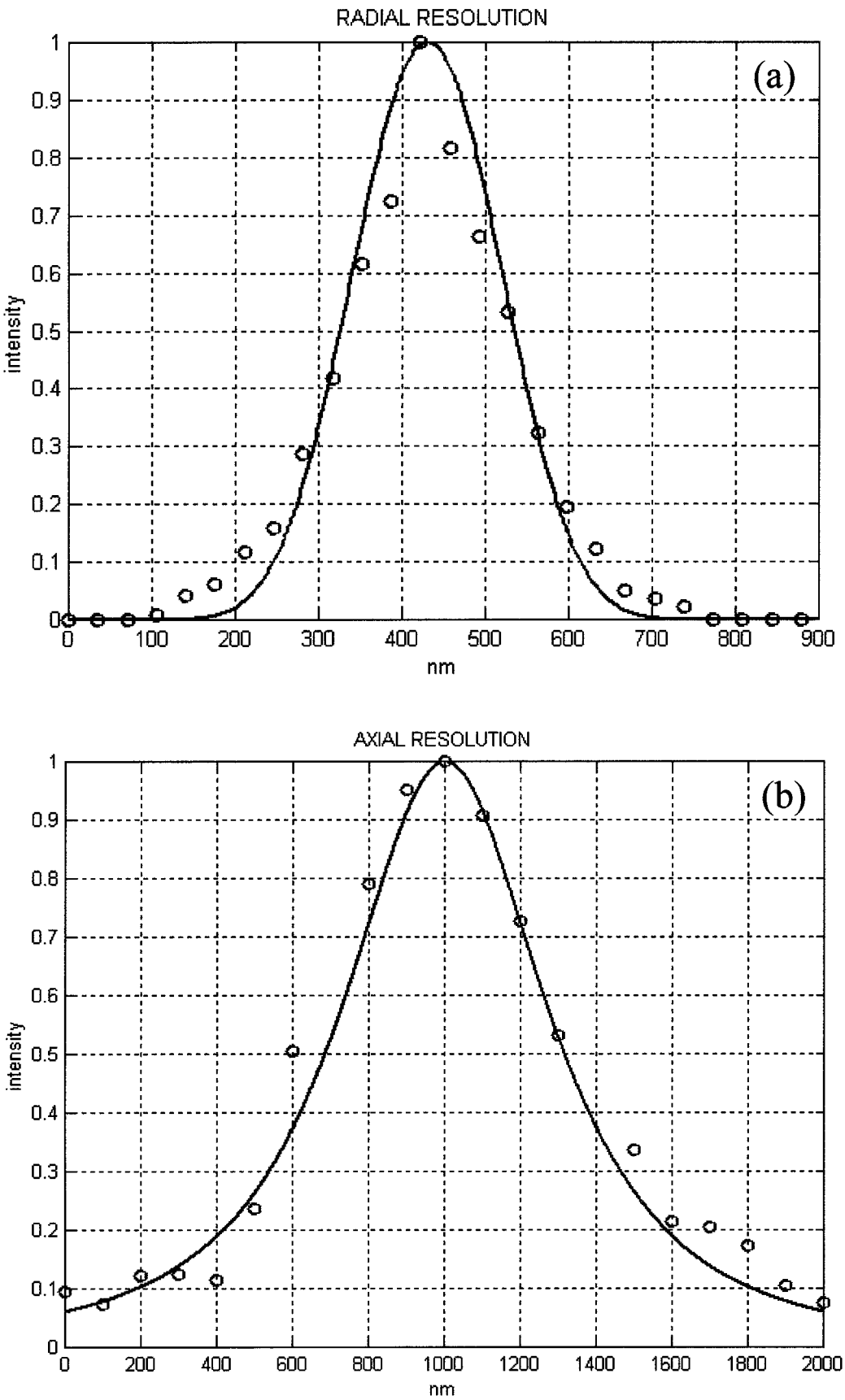

Fig. 5. The radial (**a**) and axial (**b**) intensity profiles of TPE experimental (circles) and theoretical (solid line) point spread function. See text for details.

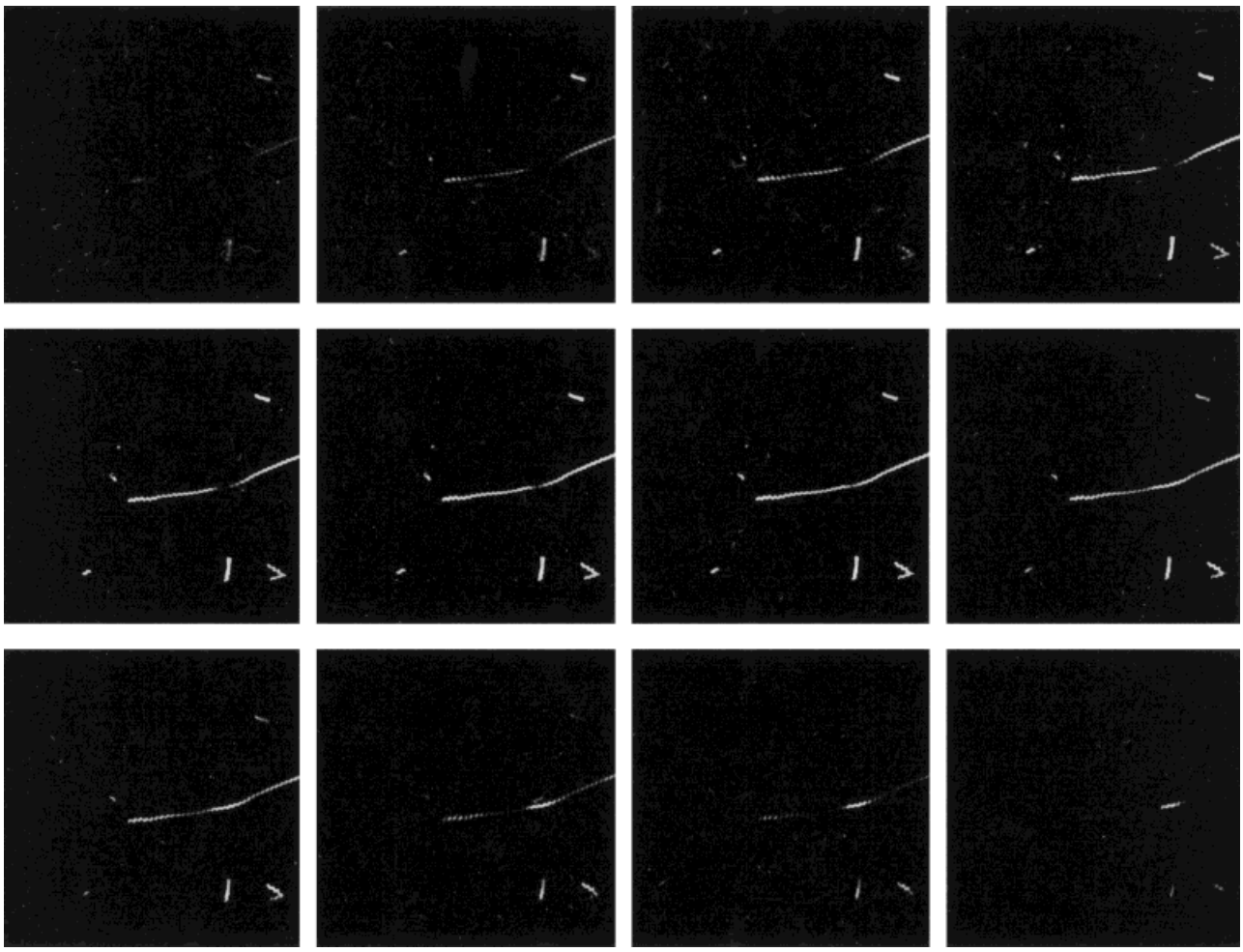

Fig. 6. An example of TPE optical sections of the structure of sperm heads of the Octopus *Eledone cirrhosa*. The sample has been fluorescently labelled with DAPI, an UV excitable DNA specific dye; see text for details. From the collection of two-dimensional images, it is possible to appreciate the very selective optical sectioning ability of the TPE microscope.

length = 43 μm. From the collection of two-dimensional images, it is possible to appreciate the very selective optical sectioning ability of the TPE microscope. The worm-like shaped sperm head is spatially organised in a 3D fashion. A view of this 3D organisation is reported in Figure 7. As in the case of 3D optical sectioning performed using conventional CLSM (Diaspro et al., 1997), the handiness can be determined only using the set of 2D slices. The most relevant visbile effect is that optical slices are independent of each other and cross-talk present in wide-field images is dramatically eliminated. This volumetric cross-talk is eliminated more than in the conventional CLSM case (Diaspro et al., 1997). The feasibility of a 3D reconstruction of such a hierarchical helically shaped structure provides the opportunity of studying a chromatin-mimer structure, too (Diaspro, 1997). In TPE, this is more relevant because it is possible to use UV excitable fluorophores like DAPI and Hoechst 33342 without the need of dangerous, under a specimen structure perspective, and problematical UV sources.

The TPE microscope has been also used with a wide range of other fluorescent molecules like Fura-2, Indo-1, $DiOC_6(3)$, fluoresceine, Texas red (data not shown). These dyes are normally excited in a single photon range from UV to green that is not always available when using CLSM.

CONCLUSION

The two-photon microscope definitively entered the arena around 1990 and is going to play a role that becomes increasingly relevant. We have built a TPE microscope utilising current commercially available main parts, i.e., infrared pulsed laser source and high quality confocal laser scanning head. The three-dimensional spatial resolution of this microscope is comparable to conventional confocal systems. However, the coupling of this technique with image restoration methods can lead to better results thanks to background noise intrinsic reduction and high signal-to-noise ratio achievable when operating in non-descanned mode. It is also worth noting the use of this

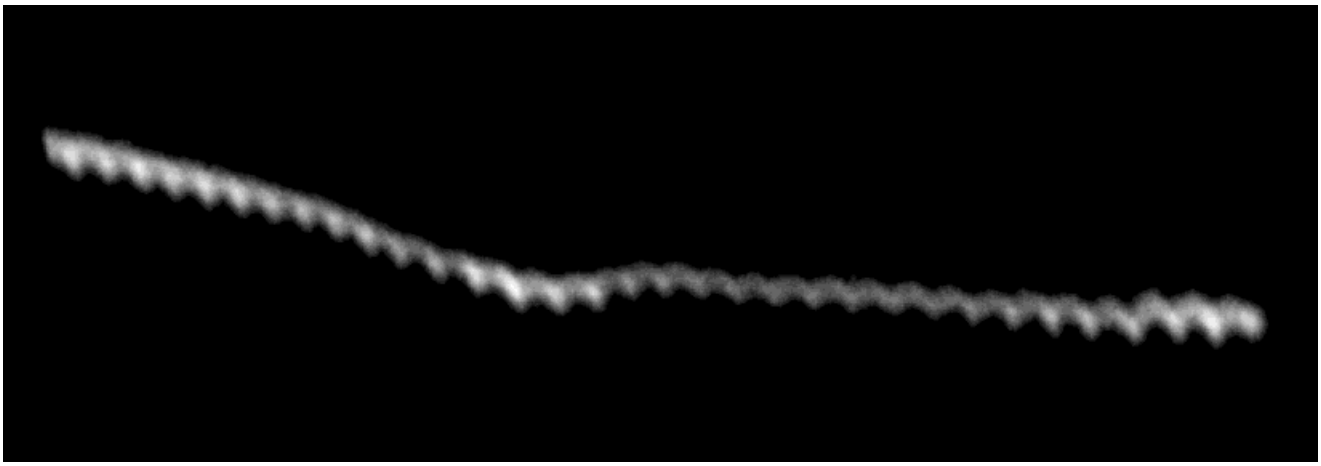

Fig. 7. The worm-like shape sperm head of the Octopus *Eledone cirrhosa* is spatially revealed in a 3D fashion.

very same TPE architecture for spectroscopic and life time studies. At present, the main disadvantages of TPE fluorescence microscopy are given by the cost of femtosecond laser sources, the lack of affordable optical fiber coupling systems, and the incomplete data on the two-photon absorption and fluorescence properties of commonly used fluorophores, and on possible thermal damage that can occur in biostructures impinged by high energy infrared radiation. We agree with Steve Potter's (1996) conclusions stating that, once technology becomes less expensive and more simple, there will not be a confocal, or a light, microscope that is not also a two-photon microscope. According to Denk and Svoboda (1997), we may conclude by stating that TPE imaging is definitely more than a gimmick.

ACKNOWLEDGMENTS

We acknowledge Hans van der Voort (Scientific Volume Imaging, Hilversum, NL), Enrico Gratton and Weiming Yu (Laboratory for Dynamic Fluorescence, Urbana-Champaign, IL), David Piston (Vanderbilt University, Nashville, TN), Peter So (MIT, Cambridge, MA), Giberto Chirico (INFM, Milan Research Unit, Italy), Bruna Barilà (INFM, Genoa Research Unit) for helpful hints, tools, and comments. We thank Cesare Fucilli for professional graphic work, and Massimo Fazio and Marco Raimondo for some useful computational tools. A special acknowledgement is for Salvatore Cannistraro and for the INFM advisory board for believing in this project.

REFERENCES

Agard DA. 1984. Optical sectioning microscopy: cellular architecture in three dimensions. Annu Rev Biophys 13:191–219.

Albota M, et al. 1998. Design of organic molecules with large two-photon absorption cross sections. Science 281:16153–1656.

Beltrame F, Diaspro A, Fato M, Martin I, Ramoino P, Sobel I. 1995. Use of stereo vision and 24-bit false colour imagery to enhance visualisation of multimodal confocal images. Proc SPIE 2412:222–229.

Benedetti P. 1998. From the histophotometer to the confocal microscope: the evolution of analytical microscopy. Eur J Histochem 42:11–17.

Bertero M, Boccacci P. 1998. Introduction to inverse problems in imaging. Philadelphia: IOP Publishing.

Born M, Wolf E. 1993. Principles of optics, 6th ed. Oxford: Pergamon.

Brakenhoff GJ, van der Voort HTM, van Spronsen EA, Nanninga N. 1986. Three-dimensional imaging by confocal scanning fluorescence microscopy. In: Somlyo AP, editor. Recent advances in electron and light optical imaging in biology and medicine. New York: Annals of the New York Academy of Sciences, vol. 483. p 405–415.

Cannell MB, Soeller C. 1997. High resolution imaging using confocal and two-photon molecular excitation microscopy. Proc R Microsc Soc 32:3–8.

Castleman KR. 1996 Digital image processing. Englewood Cliffs, NJ: Prentice Hall.

Centonze VE, White JG. 1998. Multiphoton excitation provides optical sections from deeper within scattering specimens than confocal imaging. Biophys J 75:2015–2024.

Dean P, Mascio L, Ow D, Sudar D, Mullikin J. 1990. Proposed standard for image cytometry data files. Cytometry 11:561–569.

DenkW, Svoboda K. 1997 Photon upmanship: why multiphoton imaging is more than a gimmick. Neuron 18:351–357.

Denk W, Strickler JH, Webb WW. 1990. Two-photon laser scanning fluorescence microscopy. Science 248:73–76.

Denk W, Piston D, Webb WW. 1995. Two-photon molecular excitation in laser scanning microscopy. In: Pawley JB, editor. Handbook of confocal microscopy. New York: Plenum Press, p 445–457.

Diaspro A. 1997. CLSM and SFM in the study of sperm heads of the Octopus *Eledone cirrhosa*. Microscopy and analysis (RGC) 48:9–11.

Diaspro A, Robello M. 1999. Multi-photon excitation microscopy to study biosystems. Microscopy and analysis (RGC) 58:5–7.

Diaspro A, Beltrame F, Fato M, Ramoino P. 1996. Characterizing biostructures and cellular events in 2D/3D using wide-field and confocal optical sectioning microscopy. IEEE Eng Med Biol 15:92–100.

Diaspro A, Beltrame F, Fato M, Palmeri A, Ramoino P. 1997. Studies on the structure of sperm heads of *Eledone cirrhosa* by means of CLSM linked to bioimage-oriented devices. Microsc Res Tech 36:159–164.

Diaspro A, Annunziata S, Raimondo M, Robello M. 1999 Three-dimensional optical behaviour of a confocal microscope with single illumination and detection pinhole through imaging of subresolution beads. Microsc Res Tech 45:130–131.

Gannaway JN, Sheppard CJR. 1978. Second harmonic imaging in the scanning optical microscope. Opt Quant Electron 10:435–439.

Göppert-Mayer M. 1931. Über Elementarakte mit zwei Quantensprüngen. Ann Phys 9:273–295.

Gryczynski I, Malak H, Lakowicz JR. 1996. Multiphoton excitation of the DNA stains DAPI and Hoechst. Bioimaging 4:138–148.

Gu M, Sheppard CJR. 1993. Effects of a finite sized pinhole on 3D image formation in confocal two-photon fluorescence microscopy. J Mod Opt 40:2009–2024.

Hell SW. 1996. Nonlinear optical microscopy. Bioimaging 4:121–123.

Higdon PD, Torok P, Wilson T. 1999 Imaging properties of high aperture multiphoton fluorescence scanning optical microscopes. J Microsc (OXF) 193:127–141.

Kaiser W, Garret CGB. 1961. Two-photon excitation in $CaF_2:Eu^{2+}$. Phys Rev Lett 7:229–231.
Konig K, So PTC, Mantulin WW, Gratton E. 1997. Cellular response to near-red femtosecond laser pulses in two-photon microscopes. Opt Lett 22:135–136.
Konig K, Becker TW, Fischer P, Riemann I, Halbhuber KJ. 1999. Pulse-length dependence of cellular response to intense near-infrared laser pulses in multiphoton microscopes. Optics Lett 24:113–115.
Matsumoto S, Morikawa K, Yanagida M. 1981. Light microscopic structure of DNA in solution studied by the 4',6-diamidino-2-phenylindole staining method. J Mol Biol 152:501–516.
Nakamura O. 1993 Three-dimensional imaging characteristics of laser scan fluorescence microscopy: Two-photon excitation vs. single-photon excitation. Optik 93:39–42.
Pawley JB, editor. 1995. Handbook of biological confocal microscopy. New York: Plenum Press.
Piston DW. 1999 Imaging living cells and tissues by two-photon excitation microscopy. Trends Cell Biol 9:66–69.
Potter SM. 1996. Vital imaging: two-photons are better than one. Curr Biol 6:1596–1598.
Schrader M, Hell SW, van der Voort HTM. 1996. Potential of confocal microscope to resolve in the 50–100 nm range. Appl Phys Lett 69:3644–3646.
Sheppard CJ, Kompfner R. 1978. Resonant scanning optical microscope. Appl Optics 17:2879–2885
So PTC, Berland KM, French T, Dong CY, Gratton E. 1996. Two photon fluorescence microscopy: time resolved and intensity imaging. In: Wang XF, Herman B, editors. Fluorescence imaging spectroscopy and microscopy. Chemical analysis series, vol. 137. New York: John Wiley & Sons. p 351–373.
Soeller C, Cannell MB. 1996. Construction of a two-photon microscope and optimisation of illumination pulse duration. Pflugers Arch 432:555–561.
Sytsma J, Vroom JM, De Grauw CJ, Gerritsen HC. 1998. Time-gated fluorescence lifetime imaging and microvolume spectroscopy using two-photon excitation. J Microsc 191:39–51.
van der Voort HTM, Strasters KC. 1995 Restoration of cofocal images for quantitative image analysis. J Microsc 178:165–181.
Wilson T. 1990. Confocal microscopy. London: Academic Press.
Wilson T, Sheppard CJR. 1979. Imaging and superresolution in the harmonic microscope. Opt Acta 26:761–770.
Wilson T, Sheppard CJR. 1984. Theory and practice of scanning optical microscopy. London: Academic Press.
Xu C, Webb WW. 1996. Measurement of two-photon excitation cross-sections of molecular fluorophores with data from 690 nm to 1050 nm. J Opt Soc Am B 13:481–491.